

HYDROTHERMALLY DEVELOPED TITANIUM DIOXIDE AND EUROPIUM-DOPED COMPOSITE MATERIALS FOR PHOTODEGRADATION APPLICATIONS

HIDROTERMALNI RAZVOJ TITANOVEGA OKSIDA IN Z EVROPIJEM DOPIRANI KOMPOZITNI MATERIALI ZA FOTO DEGRACIJSKE APLIKACIJE

Sasikanth S.M.* , Ganapathi Raman

Department of physics, Noorul Islam Centre For Higher Education, Kumaracoil, Tamilnadu, India. 629180

Prejem rokopisa – received: 2024-04-09; sprejem za objavo – accepted for publication: 2024-06-24

doi:10.17222/mit.2024.1151

Metal oxide nanocomposites are a critical element in nanoscale technology. Because of their many uses, a great deal of study has involved photocatalytic materials. These photocatalytic degradation characteristics also included applications like solar-cell applications. Wastewater management was included in the photodegradation property. The following study explored the development of europium tungstate nanocomposites with titanium dioxide and how they can be used in photocatalytic applications. The synthesis was conducted using the hydrothermal method and is characterized by Fourier-transform infrared spectroscopy, X-ray diffraction spectroscopy, scanning electron microscopy, and energy-dispersive spectroscopy. Application experiments were conducted using four distinct dyes, namely methyl orange, methylene blue, congo red and methyl red. The photodegradation experiments were conducted using visible light emitted by a tungsten-filament lamp. Methylene blue and methyl orange degraded to 20 % and 35 % after 1 hour respectively. After 90 min, the degradation of methylene blue went down to 15 % and congo red degraded down to 9 %. With the experiment conducted, the sample showed that it had a relatively higher photodegradation property with the dyes used. The results show that the compound had better reaction with these dyes, with a degradation down to 10 %.

Keywords: Europium, nanomaterials, organic dyes, photodegradation

Kovinski oksidi so kritični element v tehnologijah izdelave nanokompozitov. Zaradi pogoste uporabe fotokatalitičnih materialov so se avtorji tega članka odločili za študijo te vrste materialov, ki bi bili odporni proti fotodegradaciji oziroma odporni proti poškodbam zaradi učinkovanja svetlobe. Materiali za sončne celice so naprimer zelo izpostavljeni sončni svetlobi in je zato njihova odpornost proti fotodegradaciji zelo aktualna oziroma zahtevana. Tudi na področju čiščenja odpadnih vod se zahteva določena odpornost uporabljenih materialov proti poškodbam zaradi sevanja sončne svetlobe. V tem članku avtorji opisujejo razvoj nanokompozitov na osnovi volframa (W), evropija (Eu) in titanovega dioksida (TiO₂) ter ugotovljajo njihovo uporabnost za fotokatalitične aplikacije. Avtorji so sintezo nanokompozitov izvedli s hidrotermalnim postopkom. Izdelane kompozite so nato okarakterizirali s Fourierjevo transformacijsko infrardečo (FTIR) spektroskopijo, rentgensko difrakcijo (XRDS) in vrstično elektronsko mikroskopijo z energijsko disperzijsko spektroskopijo (SEM/EDS). Aplikacijske preizkuse so avtorji izvedli s pomočjo štirih različnih barvil: metil oranža, metilensko modre, kongoško rdeče in metilno rdeče. Za preizkuse fotodegradacije so uporabili vidno svetlobo, ki jo oddaja volframska žička. Metilensko modro barvilo je po eni uri degradiralo 20 %, medtem ko je metiloranž degradiral 35 %-no. Po enournem obsevanju z vidno svetlobo je metilensko modra degradirala 15 %-no in kongoško rdeča 9 %-no. S temi preizkusi so na vzorcih pokazali, da imajo izdelani kompoziti relativno dobro odpornost proti foto degradaciji z uporabljenimi barvili. Rezultati so pokazali, da spojina bolje reagira s temi barvili z degradacijo pod 10 %.

Gljučne besede: Evropij, nanomateriali, organske barve, fotodegradacija

1 INTRODUCTION

Nanomaterials are the pillars of nanoscience and nanotechnology. Researchers have developed new nanomaterials for various applications in recent years.¹ The nanomaterial's beneficial characteristics can be used in both structural and non-structural applications. It already has a huge commercial influence, which will certainly become even larger in the future. Using nanotechnology in many places all over the world can bring about various technological benefits and improved societal benefits. Nanomaterials are made up of many types of particles such as nanorods, nanotubes, nanocomposites, and

clumps. Nanocomposites are recognized as materials that transform nanosized particles into a matrix of conventional materials.² It is possible to use several materials, such as ceramics, metal and polymers, in the manufacture of this sort of material. A huge increase in the material's characteristics (e.g., mechanical strength, toughness, electrical and thermal conductivity) can be seen by adding a few components. A nanoparticle may be very successful when working in the 0.5–5 % weight range. Nanocomposites have also found frequent application in modern technological culture in line with nanomaterials.³ Applications of nanocomposites include batteries with an electrocatalyst, a lightweight material used in fuel consumption, and artificial joints that can all be made using this material's carbon-nanotube fibres. The material is

*Corresponding author's e-mail:
scholar19@niuniv.co.in (Sasikanth S. M.)

also used in food packaging, fuel tanks, films, and environmental protection, and it features capabilities like flame reaction and erosion and corrosion prevention.⁴ This material can also be used in capacitors for computer chips, and in applications like carbon nanotube battery cathodes and nanowires that are sensitive to ions. A naturally occurring clay mineral called smectite is the primary component of Bentonite.⁵ The volcanic glass in the ash is converted to clay particles during the weathering process in seawater. Bentonite is a useful adsorbent because of its wide surface area.⁶ Due to its natural abundance and lack of toxic components, bentonite clay is an environmentally responsible choice for enhancing the performance of the nanocomposite. The utilization of bentonite-modified nanocomposites in dye-removal applications has the potential to enhance the adsorption capacity and photocatalytic degradation effectiveness of harmful colours from wastewater. Consequently, this will lead to a more purified discharge and a decrease in the ecological contamination. The utilization of this synergy can enhance the effectiveness of removing a wide range of organic dyes, hence lowering the environmental impact caused by the textile and dye-production industries. The degradation mechanism is illustrated in **Figure 1**. Europium is found in the monazite sand ores containing small amounts of all the rare-earth metals.⁷ It is the most reactive of the rare-earth metals. Unlike most other rare-earth metals, europium can form stable compounds in the divalent state, Europous (Eu^{2+}) as well as the usual trivalent state, Europic (Eu^{3+}).⁸ Due to this highly reactive nature, europium compounds are selected for the synthesis of composites. The nanocomposites which are prepared now can be used for wastewater treatment using visible light with the photodegradation method.⁹

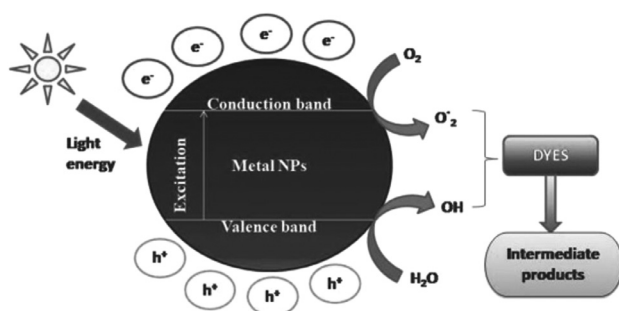
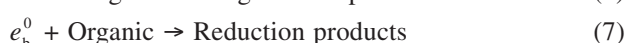
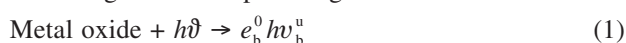


Figure 1: Photocatalytic degradation of the metal oxide nanomaterials with visible light

Electrons and +ve holes are produced in the conduction and valence bands, leading to the photon irradiation, ($h\nu$ - p) of metal oxide as per equation (1). The holes may respond straight with biological particles or indirectly through inorganic compounds equation (5) or form -OH radicals equation (3) that later corrode natural substances equation (6). Additionally, the electrons can respond with biological molecules, generating fewer products. The significance of the oxygen equation (7) was that it may respond with photogenerated electrons.

2 EXPERIMENTAL PART

The production of the europium tungstate/titanium dioxide composite utilized sodium tungstate (Na_2WO_6) as the primary ingredient. The solution consists of 0.05-M europium nitrate [$\text{Eu}(\text{NO}_3)_3$] weighing 1.65 g, 0.243g of sodium hydroxide (NaOH), 4g of titanium IV isopropoxide purchased from Sigma-Aldrich, and 100 mL of deionized water. The hydrothermal method was employed for the preparation.

2.1 Preparation of Europium Tungstate

To make the sample of europium tungstate (Eu_2WO_6), begin by dissolving 1.65g of sodium tungstate in 100 mL of deionized water. Allow the mixture to stir for 30 minutes. Following the agitation of the sample, a quantity of 0.243 g of $\text{Eu}(\text{NO}_3)_3$ was introduced into the solution of sodium tungstate at room temperature, and the solution was continuously stirred. The stirring process was continued, and the NaOH solution was gradually added drop by drop until the solution reached a pH level of 10, resulting in the complete precipitation of Eu_2WO_6 . Subsequently, filter paper was employed to refine the resultant solution. The specimen was obtained and placed in a hot-air oven following filtration, where it was maintained for a duration of 14 hours at a temperature of 110 °C. Next, the sample is subjected to calcination at a temperature of 400 °C. The final powdered sample is obtained following calcination. The furnace powder sample was collected and then underwent additional characterization operations.

2.2 Preparation of Europium Tungstate/Titanium dioxide ($\text{Eu}_2\text{WO}_6/\text{TiO}_2$)

To prepare a sample of $\text{Eu}_2\text{WO}_6/\text{TiO}_2$, the aforementioned tests are replicated and titanium IV isopropoxide is introduced during the stirring process. Following the agitation, the specimen was gathered and subsequently placed in the hot-air oven for 14 hours at a temperature of 110 °C. Next, the sample is subjected to calcination at a temperature of 400 °C. Upon completion of calcination, the resulting sample is transformed into a fine powder. The powder sample collected from the furnace underwent characterization after undergoing additional procedures.

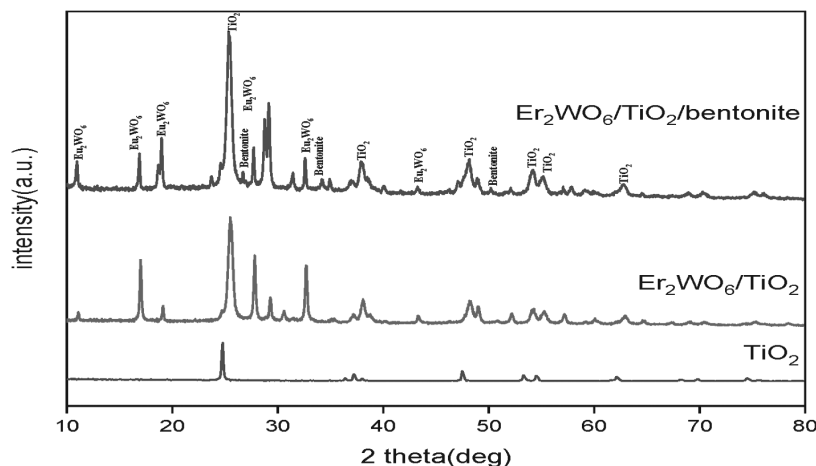


Figure 2: XRD patterns of synthesized samples

2.3 Preparation of $\text{Eu}_2\text{WO}_6/\text{TiO}_2/\text{Bentonite}$

The above experiment is repeated with the synthesis of europium tungstate/ TiO_2 and bentonite is added during the stirring process, and then the procedure is conducted as for the previous ones

2.4 Characterization Techniques

X-ray diffraction spectroscopy (XRD) experiments were conducted using the Bruker D2 Phaser instrument. XRD patterns were collected within the range of 10 to 80 degrees (2θ). BRUKER Alpha T, Germany, was used to acquire Fourier-transform spectroscopy (FTIR) spectra in the range 550–4000 cm^{-1} . An examination employing scanning electron microscopy (SEM) was conducted utilising a field-emission gun SEM (JSM-7600F, Japan) operating at an accelerating voltage of 10 kV. The produced nanomaterials undergo photodegradation using a visible light apparatus equipped with a tungsten-filament lamp and a cooling mechanism to maintain a constant temperature during the experiment.

3 RESULTS

3.1 X-ray diffraction Analysis

The XRD examination was performed on the produced samples, and the results are presented in **Figure 2**. According to the spectrum data of the sample, the diffraction peaks for TiO_2 are observed at specific angles: 27.32°, 36.85°, 44.36°, 54.88°, 56.85°, and 62.74°. These angles correspond to the crystallographic planes 110, 101, 210, 211, 220, and 002, respectively. These findings are consistent with the information provided in the JCPDS file number 89-8304. Based on the spectra obtained from the sample, the diffraction peaks of Eu_2WO_6 are observed at specific 2θ values: 13.84, 28.26, 33.83, and 46.84. These peaks correspond to the 100, 200, 111, and 002 planes, respectively, for the monoclinic and hexagonal phases as documented in the JCPDS file number 33-1387. The material's crystal prop-

erty can be defined by the values $K_{\alpha 1}=1.54060$, $K_{\alpha 2}=1.54443$ and $K_{\beta}=1.39225$. The XRD patterns depicting the characteristics of the bentonite nanoparticles are in **Figure 2**. The diffraction peaks seen at angles $2\theta = 26.52^\circ$, 36.36° , and 50.78° correspond to the crystal planes (210), (124), and (144) of the bentonite material. The XRD patterns closely match the standard JCPDS file (card no.01-088-0891). By employing the value 2θ as a reference, the particle size of the material can be determined using Debye-Scherrer's equation, yielding a result of 42.85 nm.

3.2 Fourier-Transform Infrared Spectroscopy Analysis

Figure 3 illustrates the relationship between the assigned frequencies and the frequency of observation by FTIR spectroscopy. The europium tungstate sample exhibits absorption peaks at 3543 cm^{-1} and 2987 cm^{-1} . Typically, metal oxides have an absorption band below 1000 cm^{-1} , which is caused by interatomic vibrations. The determination of the sample's most intense absorption band is possible. The wave numbers 3543 cm^{-1} and 1579 cm^{-1} indicate the presence of the O-H stretching

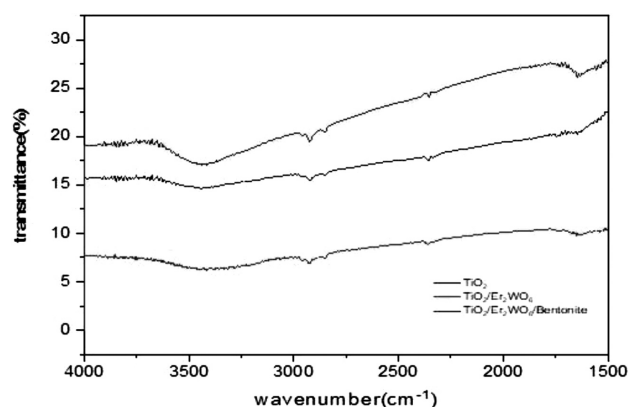


Figure 3: FTIR spectra of prepared samples

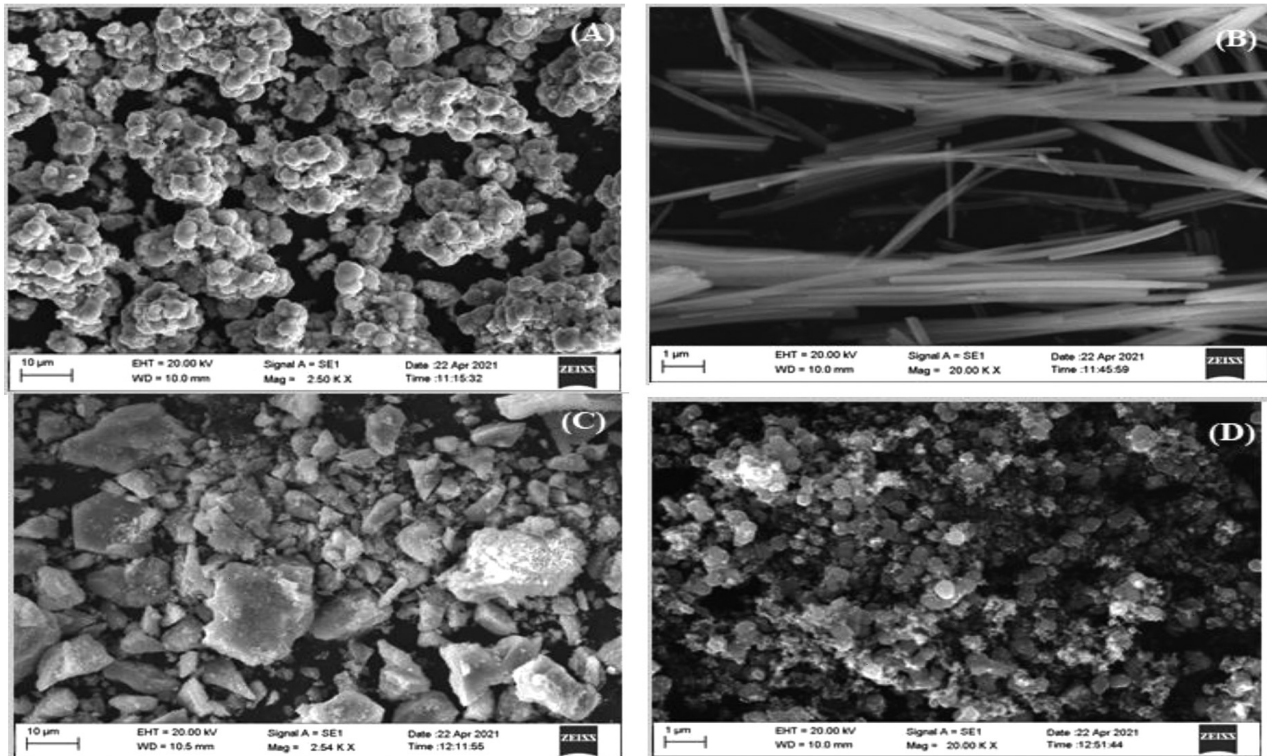


Figure 4: SEM of (A) TiO_2 , (B) Er_2WO_6 , (C) $\text{Er}_2\text{WO}_6/\text{TiO}_2$, (D) $\text{Er}_2\text{WO}_6/\text{TiO}_2/\text{bentonite}$

band. The presence of tungstate oxide in the europium-doped tungstate oxide nanoparticles is verified by this evidence.¹⁰

3.3 Scanning Electron Microscopy/Energy Dispersive Spectroscopy

Using a scanning electron microscope, the morphological structure of the sample was examined. The mate-

rial was placed on aluminium stubs inside the chamber and analysed using this equipment. The images are shown in Figure 4. The images of the surface changes in europium tungstate oxide nanocomposites were obtained using a high acceleration voltage, as shown by the results with TiO_2 compounds. The sample's mean particle size is calculated to be 43.2 from the SEM micrograph. The chemical elements present in a sample can be identified

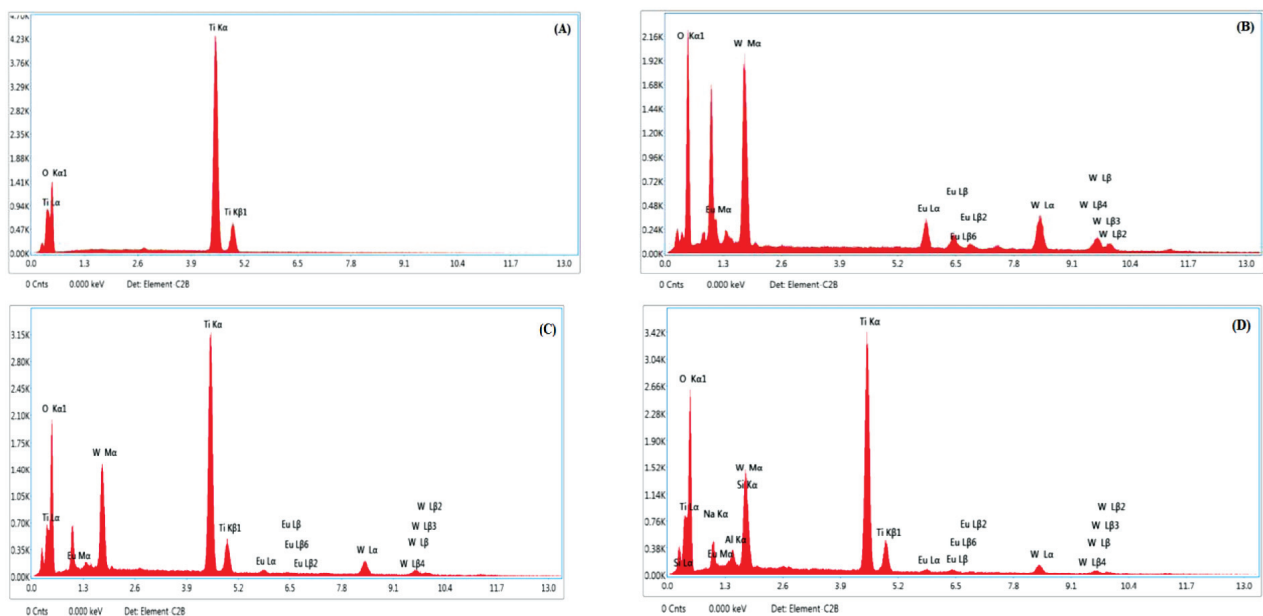


Figure 5: EDS of (A) TiO_2 , (B) Er_2WO_6 , (C) $\text{Er}_2\text{WO}_6/\text{TiO}_2$, (D) $\text{Er}_2\text{WO}_6/\text{TiO}_2/\text{bentonite}$

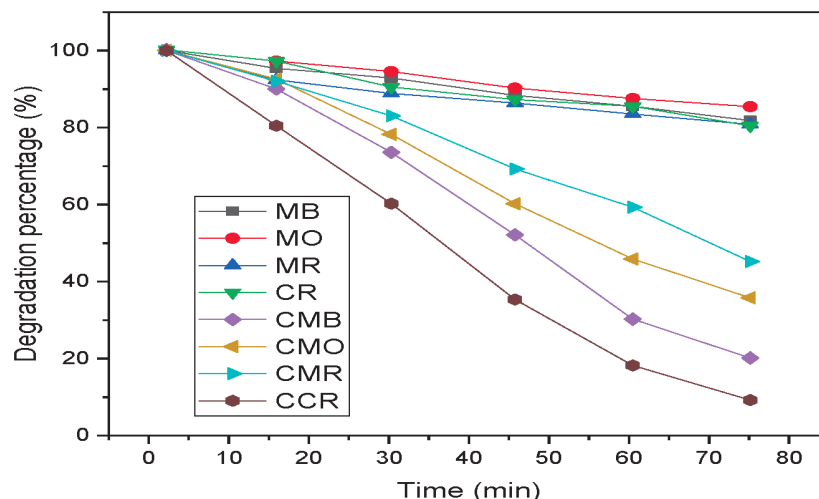


Figure 6: Degradation of four different dyes with and without catalyst

and their relative abundance can be estimated using energy-dispersive spectroscopy (EDS), as shown in **Figure 5**. Metal multi-layer coating thickness measurements and alloy analysis is made using EDS.^{11–13}

3.4 Photodegradation Studies

Photodegradation experiments were conducted using visible-light exposure (tungsten-filament lamp). Here, four different dyes, specifically methyl orange, methylene blue, congo red, and methyl red, are utilized. The degradation of all the colours occurred both in the presence and absence of the nanocomposites. **Figure 6** depicts the outcome of the four dyes prior to and following irradiation with a catalyst. The results demonstrated that the produced nanocatalyst consistently accelerates the degradation process by reducing the degradation time by half. **Figure 6** displays the degradation graph of the dyes, both with and without the catalyst. The dye degradation % can be calculated using the formula:

$$D = \frac{C_0 - C}{C_0} \times 100$$

where C_0 is the initial concentration of the dye and C is the final concentration.

The compounds are MB – Methylene blue, MR – methyl red, MO – methyl orange, CR – congo red, CMB – compound with methylene blue, CMO – compound with methyl orange, CMR – compound with methyl red and CCR – compound with congo red. From the graph, methylene blue and methyl orange have degraded to 20 % and 35 % after 1 hour, respectively. After 75 min, degradation of methylene blue has gone to 15 % and congo red has degraded down to 9 %.^{14–18}

4 DISCUSSION

This study investigates the synthesis and application of nanocomposites of europium tungstate and TiO_2 for

photocatalytic activities. The nanocomposite was synthesised and characterised using X-ray diffraction (XRD), Fourier-transform infrared spectroscopy (FTIR), scanning electron microscopy (SEM), and energy-dispersive X-ray spectroscopy (EDS) techniques. The nanocomposite additionally incorporated bentonite clay, which augmented the degradation % as a result of its notable absorption ability.^{19,20}

5 CONCLUSIONS

The success of nanotechnology strongly depends on the utilization of metal oxide nanocomposites. This paper focuses on the synthesis and utilization of Europium tungstate nanocomposites with TiO_2 in photocatalytic processes. The effective synthesis of the nanocomposite was confirmed through characterizations using XRD, FTIR, SEM and EDS. The addition of bentonite clay, which has a high absorption capacity, has resulted in an increase in the degradation %. The incorporation of bentonite clay into europium tungstate/titanium dioxide ($\text{Eu}_2(\text{WO}_4)_3/\text{TiO}_2$) nanocomposites has consequences for the enhancement of the material's structure, catalytic characteristics, and environmental applications. Bentonite clay, which is well-known for its large surface area and remarkable adsorptive properties, possesses the capability to improve the dispersion and stability of the nanocomposite particles, which ultimately leads to the production of catalytic sites that are more uniform and effective. An increase in the photocatalytic efficacy of TiO_2 can be achieved through the enhancement of light absorption and the facilitation of charge separation. This can lead to an improvement in the breakdown of organic pollutants in water and air-purification processes. In addition, the mechanical strength and thermal stability of the nanocomposite can be improved, which will result in an increase in its durability throughout the operation. Because they contain bentonite, ($\text{Eu}_2(\text{WO}_4)_3/\text{TiO}_2$) nanocomposites have the potential to provide an alternative to

conventional additives that is both more cost-effective and less harmful to the environment. The potential uses of these nanocomposites in areas such as waste management, environmental remediation and advanced material manufacture are expanded as a result of this. Two distinct dyes were utilized in the degradation procedure. Methylene blue and methyl orange degraded to 20 % and 35 % after 1 hour respectively. After 90 min, the degradation of methylene blue was down to 15 % and congo red degraded down to 9 %. With the experiment conducted, the samples have shown that it has relatively higher photodegradation property with the dyes used. This proves that different dye degradation can be achieved with this compound.

6 REFERENCES

- ¹ Y. N. Rajeev, C. M. Magdalane, S. Hepsibha, G. Ramalingam, B. A. Kumar, L. B. Kumar, S. Sambasivam, Europium decorated hierarchical TiO₂ heterojunction nanostructure with enhanced UV light photocatalytic activity for degradation of toxic industrial effluent, *In.Chem Comms*, 157, (2023), 111339, doi:10.1016/j.inoche.2023.111339
- ² B. Bethi, S. H. Sonawane, B. A. Bhanvase, S. P. Gumfekar, Nanomaterials-based advanced oxidation processes for wastewater treatment: A review, *Chem. Eng. Process. Process Intensif.*, 109 (2016), 178–189, doi:10.1016/j.cep.2016.08.016
- ³ R. Ahmad, Z. Ahmad, A. U. Khan, N. R. Mastoi, M. Aslam, J. Kim, Photocatalytic systems as an advanced environmental remediation: Recent developments, limitations and new avenues for applications, *J. Environ. Chem. Eng.*, 4 (2016), 4143–4164, doi:10.1016/j.jece.2016.09.009
- ⁴ Z. Xiu, M. Guo, T. Zhao, K. Pan, Z. Xing, Z. Li, Recent advances in Ti³⁺ self-doped nanostructured TiO₂ visible light photocatalysts for environmental and energy applications, *Chem. Eng. J.*, 382 (2020), 123011, doi:10.1016/j.cej.2019.123011
- ⁵ E. Rossetto, D. I. Petkowicz, J. H. Z. dos Santos, S. B. C. Pergher, F. G. Penha, Bentonites impregnated with TiO₂ for photodegradation of methylene blue, *Appl. Clay Sci.*, 48 (2010), 602–606, doi:10.1016/j.heliyon.2017.e00488
- ⁶ W. L. Feng, X. Qin, P. Su, Synthesis, photoluminescence and theoretical explanations of trivalent europium-doped dipotassium tungstate phosphors, *Optik*, 131 (2017), 1007–1015, doi:10.1016/j.ijleo.2016.12.017
- ⁷ D. H. Templeton, A. Zalkin, Crystal structure of europium tungstate, *Acta Crystallogr.*, 16 (2002), 762–766, doi:10.1107/S0365110X63001985
- ⁸ Parul, K. Kaur, R. Badru, P. P. Singh, S. Kaushal, Photodegradation of organic pollutants using heterojunctions: A review, *J. Environ. Chem. Eng.*, 8 (2020), 103666, doi:10.1016/j.jece.2020.103666
- ⁹ A. Safarzadeh-Amiri, J. R. Bolton, S. R. Cater, Ferrioxalate-mediated photodegradation of organic pollutants in contaminated water, *Water Res.*, 31 (1997), 787–798, doi:10.1016/S0043-1354(96)00373-9
- ¹⁰ X. Gong, P. Wu, W. K. Chan, W. Chen, Effect of γ -ray irradiation on structures and luminescent properties of nanocrystalline MSO₄: J. *Phys. Chem. Solids.*, 61 (2000), 115–121, doi:10.1016/S0022-3697(99)00223-1
- ¹¹ G. Tian, H. Fu, L. Jing, C. Tian, Synthesis and photocatalytic activity of stable nanocrystalline TiO₂ with high crystallinity and large surface area, *J. Hazard. Mater.*, 161 (2009), 1122–1130, doi:10.1016/j.jhazmat.2008.04.065
- ¹² T. Butburee, Y. Bai, H. Wang, H. Chen, Z. Wang, G. Liu, et al., 2D Porous TiO₂ Single-Crystalline Nanostructure Demonstrating High Photo-Electrochemical Water Splitting Performance, *Adv. Mater.*, 30 (2018), doi:10.1002/adma.201705666
- ¹³ Z. Zarhri, M. Á. Avilés Cardos, Y. Ziat, M. Hammi, O. el Rhazouani, J. C. Cruz Argüello, et al., Synthesis, structural and crystal size effect on the optical properties of sprayed TiO₂ thin films: Experiment and DFT TB-mbj, *J. Alloys Compd.*, 819 (2020), doi:10.1016/j.jallcom.2019.153010
- ¹⁴ E. Kusiak-Nejman, A. W. Morawski, TiO₂/graphene-based nanocomposites for water treatment: A brief overview of charge carrier transfer, antimicrobial and photocatalytic performance, *Appl. Catal. B Environ.*, 253 (2019), 179–186, doi:10.1016/j.apcatb.2019.04.055
- ¹⁵ V. Kumar Pandey, C. K. Dixit, G. P. Shukla, C. K. Pandey, Study of Surface Morphology of TiO₂-SnO₂ Nanocomposites, *Mater. Today Proc.*, 24 (2020), 960–965, doi:10.1016/j.matpr.2020.04.408
- ¹⁶ F. Anaya-Rodríguez, J. C. Durán-Álvarez, K. T. Drisya, R. Zanella, The challenges of integrating the principles of green chemistry and green engineering to heterogeneous photocatalysis to treat water and produce green H₂, *Catalysts*, 13 (2023), 154, doi:10.3390/catal13010154
- ¹⁷ D. Cai, S. Yang, Z. Ma, L. Liu, D. Wang, J. Qian, Y. Li, Enhancement of charge transfer rate at mixed morphology TiO₂/graphene interface by Al³⁺, *Mater. Today Chem.*, 27 (2023), 101325, doi:10.1016/j.mtchem.2022.101325
- ¹⁸ A. A. Aboud, N. S. Abd El-Gawaad, M. Al-Dossari, Physical Properties of Cu, Co, and Zn doped TiO₂ nanocrystalline thin films prepared using spray pyrolysis, *Phys. Scr.*, 99 (2023), 015937, doi:10.1088/1402-4896/ad14de
- ¹⁹ N. Thakur, N. Thakur, K. Kumar, V. Arya, A. Kumar, Encapsulation of *Tinospora cordifolia* plant in Ni doped TiO₂ nanoparticles for the degradation of malachite green dye, *Nanofabrication*, 8 (2023), doi:10.37819/nanofab.8.305
- ²⁰ P. Zhao, Y. Yang, Y. Pei, X. Luo, TEMPO-oxidized cellulose beads embedded with Au-doped TiO₂ nanoparticles for photocatalytic degradation of Tylosin, *Cellulose*, 30 (2023), 1133–1147, doi:10.1007/s10570-022-04935-6